Journal of Applied Physics

Dominant defects and carrier transport in single crystalline cuprous oxide: A new attribution of optical transitions

Cite as: J. Appl. Phys. **130**, 175701 (2021); https://doi.org/10.1063/5.0059406
Submitted: 09 June 2021 • Accepted: 07 October 2021 • Published Online: 01 November 2021

M. Nyborg, Ilia Kolevatov, G. C. Vásquez, et al.

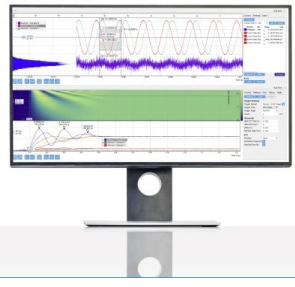

Journal of Applied Physics ARTICLE scitation.org/journal/jap

Dominant defects and carrier transport in single crystalline cuprous oxide: A new attribution of optical transitions

Cite as: J. Appl. Phys. **130**, 175701 (2021); doi: 10.1063/5.0059406
Submitted: 9 June 2021 · Accepted: 7 October 2021 ·
Published Online: 1 November 2021

M. Nyborg,[1,a)] Ilia Kolevatov,[1,2] G. C. Vásquez,[1] K. Bergum,[1] and E. Monakhov[1,a)]

AFFILIATIONS

[1]Department of Physics/Centre for Materials Science and Nanotechnology, University of Oslo, P.O. Box 1048 Blindern, Oslo N-0316, Norway
[2]Justervesenet, P.O. Box 170, Kjeller N-2007, Norway

[a)]**Authors to whom correspondence should be addressed:** martin.nyborg@fys.uio.no and eduard.monakhov@fys.uio.no

ABSTRACT

Electronic properties of single crystal (111) Cu_2O wafers have been investigated using a number of complementary techniques. Secondary ion mass spectrometry has shown significant presence of hydrogen and nitrogen. Cathodoluminescence measurements reveal strong near-band emission indicating the good electronic quality of the wafers. Two deep emission lines are observed at 1.3 and 1.7 eV. Temperature-dependent Hall effect measurements reveal electronic levels at around $E_V + 0.16$ eV, $E_V + 0.22$ eV, and $\sim E_V + 0.4$ eV, where E_V is the valence band edge. The discussion on the identity of the electronic centers calls for a revision of the traditional assignments of the 1.3-eV and 1.7-eV lines in order to take into account independent theoretical predictions. The temperature dependence of carrier mobility shows that the mechanism limiting the mobility can be described by scattering on neutral and ionized defect centers.

I. INTRODUCTION

Cuprous oxide (Cu_2O) is a direct bandgap semiconductor with a bandgap of ~2.17 eV.[1–3] It has been intensively studied for its promising properties for photovoltaic applications due to the abundance and non-toxicity, strong light absorption, and the possibility of thin-film processing. However, efficiencies for most thin-film devices have yet to surpass ~2%.[2] On the other hand, solar cells based on oxidized copper sheets have achieved efficiencies as high as 8%.[4] The challenge to achieve higher efficiencies is believed to be due to the inability to fully control defect concentrations in Cu_2O, where the excess acceptor concentrations are normally attributed to non-stoichiometry caused by cation deficiency through copper vacancies (V_{Cu}).[3]

Theoretical predictions on the properties of V_{Cu} by the density functional theory (DFT) are somewhat contradicting. According to Raebiger *et al.*,[5] V_{Cu} can have another configuration, the so-called split vacancy ($V_{Cu,split}$), that has higher formation energy for both neutral and negative charge states. $V_{Cu,split}$ is thus expected to be less energetically favorable. Both the configurations are predicted to have the acceptor transition (0/−) at around $E_V + 0.28$ eV, where E_V is the valence band edge. Later, Scanlon *et al.*[6] have estimated that neutral $V_{Cu}(0)$ and $V_{Cu,split}(0)$ have similar formation energies, which is in contrast to the calculations by Raebiger *et al.*[5] According to Scanlon *et al.*,[6] the acceptor transitions (0/−) for V_{Cu} and $V_{Cu,split}$ occur at $E_V + 0.23$ eV and $E_V + 0.47$ eV, respectively. One can see that both Raebiger *et al.*[5] and Scanlon *et al.*[6] agree on the preferred configuration for the negative charge state, while disagreeing somewhat on the relation between the formation energies for the neutral charge state.

Experimental studies on electronic properties of nominally intrinsic Cu_2O have routinely reported dominant acceptor levels around 0.2 eV and around 0.4–0.5 eV above E_V (see recent Refs. 7–10 and references therein). Over the decades, there have been a number of different identifications of these levels. Since the results were obtained for nominally intrinsic Cu_2O, the identifications were normally attributed to intrinsic defects, mostly to vacancy related defects. For instance, Paul *et al.*[7] have attributed the electronic level at $E_V + 0.45$ eV to a Cu-monovacancy and the level at $E_V + 0.25$ eV to a Cu-divacancy. After the DFT studies by Raebiger *et al.*[5] and

Scanlon *et al.*,[6] the assignments tend to involve V_{Cu} and $V_{Cu,split}$. One can notice, however, that the effect of unintentional impurities has not been seriously considered and investigated.

Nitrogen is one of the most established acceptor dopants in Cu_2O. Nitrogen substituting oxygen (N_O) is routinely assigned to a shallow acceptor level at 0.12–0.18 eV above E_V.[11–13] This range is in agreement with the estimate based on the effective mass approximation, which gives a theoretical activation energy of 0.16 eV.[11] However, recent DFT calculations could not place N_O as a shallow acceptor. It was reported to have a deeper level at $\sim E_V + 0.5$ eV, making it a less likely candidate as a dominant shallow acceptor in Cu_2O (see recent Ref. 14 and references therein). Instead, nitrogen is proposed to mainly replace Cu in its molecular form, as $(N_2)_{Cu}$,[14] which is supported by experimental results showing that nitrogen is present in Cu_2O predominantly as N_2.[15] Finally, it is calculated that $(N_2)_{Cu}$ has a shallower acceptor level at ~0.2 eV.[16] It is interesting to note that Malerba *et al.*[17] have shown direct evidence of optical absorption around 0.5–0.7 eV associated with nitrogen induced electronic levels. This observation is consistent with the DFT results on the acceptor level of N_O at $\sim E_V + 0.5$ eV.[14]

Although hydrogen is known to be an abundant impurity in oxides, our understanding of its properties in Cu_2O is limited. According to Van de Walle and Neugebauer[18] isolated interstitial hydrogen (H_i) is a negative-U center in various semiconductors. It has been calculated that the positive charge state, $H_i(+)$, tends to take the bond-centered (BC) configuration, while the negative charge state, $H_i(-)$, tends to take the tetrahedral (tet) configuration. The negative-U behavior is thus attributed to the electronic and structural transition between $H_{i,BC}(+)$ and $H_{i,tet}(-)$. The calculations suggest that for the majority of semiconductors, the electronic level for the transition between $H_{i,BC}(+)$ and $H_{i,tet}(-)$ is universally aligned with respect to the vacuum level. The DFT calculations put this level at around 4.5 eV below the vacuum level.[18] Adopting this hypothesis and taking the electron affinity of Cu_2O as 3.1 eV,[2,3] one can estimate that the expected level in Cu_2O is at ~1.4 eV below the conduction band (E_C) or at ~0.8 eV above E_V.

First, DFT calculations on some hydrogen-related complexes have been reported by Scanlon and Watson.[19] Several possible atomic configurations for H_i have been calculated, including tetrahedral, octahedral, bond-centered, and anti-bonding configurations. Unfortunately, the transition between $H_{i,BC}(+)$ and $H_{i,tet}(-)$ has not been explicitly considered, and the hypothesis on the universal alignment has not been explicitly checked for Cu_2O. The calculations by Scanlon and Watson[19] have also demonstrated the ability of hydrogen to passivate V_{Cu}. The hydrogen-V_{Cu} complex (H-V_{Cu}) has been shown to have the lowest formation energy among the considered complexes. It is predicted to have the donor level (+/0) at around $E_V + 0.1$ eV and the acceptor level (0/−) at around $E_V + 1.2$ eV.

The experimental reports on the role of hydrogen in Cu_2O are quite scarce. Hering *et al.*[20] have reported on improved carrier transport properties when hydrogen is introduced during Cu_2O deposition by magnetron sputtering. This is attributed to hydrogen passivating donor-like states, resulting in improved mobility in the films. The study also highlights an increase in acceptor ionization energy with higher hydrogen flow during growth, which can be interpreted as the appearance of a hydrogen-related defect with higher activation energy. Tabuchi and Matsumura[21] and Kumar *et al.*[22] also report on improved mobility in hydrogen enriched Cu_2O. The increased mobility is accompanied by a decrease in carrier concentration, which suggests either passivation of acceptors by hydrogen or an increase in the acceptor activation energy. These findings are consistent with theoretical predictions on hydrogen passivation of vacancies by Scanlon and Watson.[19]

The literature shows that the majority of studies are performed on magnetron-sputtered films or thermally oxidized copper sheets. In this work, we report on the dominant electronic states in single crystalline Cu_2O. We employ a number of complementary techniques to establish and identify the dominant electronic states.

II. EXPERIMENTAL DETAILS

Two commercially available natural single crystal Cu_2O wafers from SurfaceNET with a resistivity of 20 kΩ cm were used in the study. The wafers had (111)-orientation and a size of 1×1 cm^2 with a thickness of 500 μm. One of the wafers was measured by x-ray diffraction (XRD) before it was cut into smaller samples for Schottky diode fabrication, Secondary Ion Mass Spectrometry (SIMS), and Cathodoluminescence (CL) measurments. Another wafer was used for the temperature-dependent Hall (TDH).

SIMS measurements of hydrogen and nitrogen concentrations were conducted in a Cameca IMS7f microanalyzer with Cs^+ primary ions at 15 keV. Reference samples were used to quantify the concentrations in the Cu_2O wafers studied. The reference samples used were magnetron sputtered, phase-pure Cu_2O films ion-implanted with known doses of hydrogen and nitrogen. The implantation of hydrogen was performed with an energy of 20 keV and a dose of 1×10^{16} cm^{-2}. These implantation conditions resulted in a hydrogen profile with a peak concentration of 8×10^{20} cm^{-3} at a depth of ~160 nm. The implantation of nitrogen was done with the same dose 1×10^{16} cm^{-2} and an ion energy of 80 keV. This energy was chosen in order to provide a nitrogen depth profile similar to that of hydrogen. The resulting nitrogen profile has a peak concentration of 8×10^{20} cm^{-3} at a depth of ~120 nm. The SIMS measurements were carried out for the reference samples and the studied single crystalline wafers at the same measurement conditions on the same day. The count rates of the secondary ions were then calibrated using the reference samples. This calibration was used to deduce the concentrations from the rate counts for the analyzed single crystal samples. The measurements revealed a high concentration of hydrogen in the Cu_2O wafers: as high as 3×10^{19} cm^{-3}. Nitrogen concentration was established to be $\sim 7 \times 10^{17}$ cm^{-3}.

Structural characterization was performed using X-ray Diffraction (XRD) in a Bragg–Brentano geometry and $CuK_{\alpha 1}$ radiation selected by a GE(002) asymmetric monochromator on the primary beam side. The scans were performed in a Bruker AXS D8 Discovery XRD system.

CL was studied with a JEOL JSM-IT300 SEM with a Delmic SPARC CL system equipped with an Andor Shamrock SR-193i spectrometer, a 300 l/mm grating, and a charged couple device (CCD) Andor Newton DU940P-BU2, allowing us to achieve 0.97 nm spectral resolution. The CL spectra were recorded at 80 K with acceleration voltages of 3, 5, 10, and 20 keV and a probing current of 100 pA.

Free carrier density has been assessed by TDH measurements conducted with two different Lakeshore 7604 setups, one configured for low-temperature measurements (20–300 K) and one for high temperature (300–700 K). The sample was first measured in the low-temperature setup at 120–300 K, subsequently, it was measured in the high temperature setup at 300–550 K.

Circular Al contacts with a diameter of 0.5 mm were deposited by thermal evaporation through a shadow mask. Subsequently, Au was deposited over the whole backside surface as the back contact. This resulted in Schottky diodes with rectifications of ∼2 orders of magnitude. Thermal admittance spectroscopy (TAS) was performed under 1 V reverse bias with an Agilent 4280A LCR meter with probe frequencies between 10 kHz and 1 MHz and 20 mV amplitude.

III. RESULTS AND DISCUSSION

The XRD pattern of a θ–2θ scan (Fig. 1) reveals two dominant peaks at 36.43° and 77.35°. The peaks correspond to diffraction at (111) and (222) planes of Cu_2O. This confirms phase-pure, single crystalline Cu_2O with the orientation along the [111] direction. The lattice constant $a = 4.269 \pm 0.004$ Å was obtained from the position of the [111] reflection and is in good agreement with the literature value of 4.270 ± 0.001 Å.[3] The two minor peaks marked by asterisks originate from the Al sample holder. One can also observe an indication of a minor peak at ∼33°. At the moment, we cannot make a conclusive claim on the origin of this peak. One can speculate that it can be due to (110) CuO since the presence of CuO inclusions or a thin CuO surface layer cannot be excluded.[23] On the other hand, we do not observe the diffraction on (220) CuO, expected at ∼70° with a similar intensity.

Figure 2 depicts CL spectra measured at 80 K with different electron-beam energies, the spectra are consistent with each other and indicate good crystal quality and uniformity. The spectra reveal strong and sharp near-band emission (NBE) lines in the photon energy range 1.9–2.1 eV. In addition, two broad, strong luminescence bands are observed at around 1.3 and 1.7 eV.

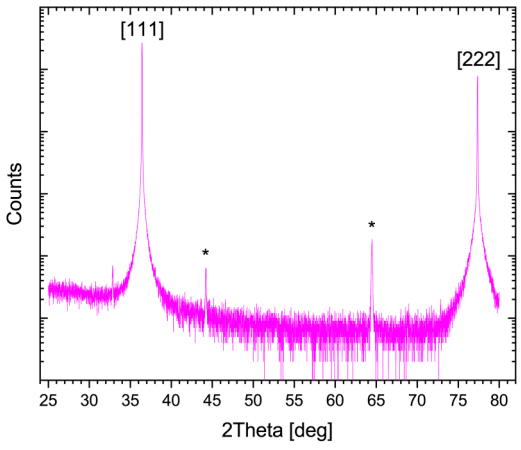

FIG. 1. θ-2θ XRD scan for the Cu_2O sample. Asterisks denote minor peaks that originate from the sample holder.

Similar transitions were routinely observed by photoluminescence (PL) already over half a century ago (see Ref. 24 and references therein). First tentative identification was put forward by Bloem *et al.*,[24] where the luminescence peak at ∼1.2–1.3 eV was attributed to the acceptor state of V_{Cu}, and the peak at ∼1.7 eV was assigned to a donor state of oxygen vacancy (V_O). Later, Gastev *et al.*[25] assigned the emission at ∼1.7 eV to a double donor state of oxygen vacancy (V_O^{2+}), which was based on previous studies by Zouaghi *et al.*[26] using infrared absorption and photoconductivity. Since then, this identification has been routinely repeated in the literature (see Refs. 2 and 3 and references therein). Apparently, these identifications contradict the DFT studies by both Raebring *et al.*[5] and Scalon *et al.*[6,19] First, V_O is predicted to be electrically neutral without electronic levels in the bandgap.[5,6,19] Second, the assignment of the 1.3-eV peak to V_{Cu} would imply that the acceptor level of V_{Cu} is at $E_V + 0.8$ eV, which also contradicts to the DFT predictions.[5,6,19]

Based on the DFT calculations, one can put forward another identification of the deep emission lines. The photon energy 1.3 eV is close to the energy for the acceptor level of H-V_{Cu}, which was put by Scanlon and Watson[19] at $\sim E_V + 1.2$ eV. Since hydrogen is abundant in the studied samples, as shown by SIMS, it is tempting to attribute the 1.3-eV emission line to H-V_{Cu}. The 1.7-eV emission line can be tentatively attributed to the acceptor transition of $V_{Cu,split}$ that is predicted to have the level at $E_V + 0.47$ eV,[6,19] i.e., at $\sim E_C - 1.7$ eV. The latter identification would then imply that either (i) $V_{Cu,split}$ is the preferred and dominant configuration compared to V_{Cu} or (ii) the radiative transition for $V_{Cu,split}$ is significantly more efficient compared to that for V_{Cu}.

Five different NBE peaks can be detected in the CL spectra and labeled as peaks 1–5 (Fig. 2). One can observe that the shape of the NBE in the present experiment is quite similar to that reported previously for high-quality Cu_2O films with photoluminescence (PL).[27] This leads to a peak identification similar to that in Ref. 27. The separation between peaks 4 and 5 is 0.025 eV, which is in good agreement with the PL data.[27] The peaks are, thus, identified as the orthoexcitonic (X_o) emission coupled with absorption or emission of the Γ^-_{12} phonon, where peak 5 at 2.043 eV is attributed to the absorption of the phonon ($X_o + \Gamma^-_{12}$) and peak 4 at 2.018 eV is due to the emission ($X_o - \Gamma^-_{12}$). Since the energy of the Γ^-_{12} phonon is 0.0125 eV, one can deduce the phonon-free X_o emission energy as the center point between peaks 4 and 5, which is 2.030 eV. Taking the exciton binding energy 0.14 eV[28] results in a bandgap of 2.17 eV at 80 K. Peak 3 at 1.974 eV is 0.056 eV below the X_o emission, which is close to the Γ^+_{25} phonon energy reported at 0.064 eV.[29] Hence, we identify peak 3 as X_o coupled with emission of the Γ^+_{25} phonon ($X_o - \Gamma^+_{25}$). Similarly, peak 2 at 1.950 eV is identified as X_o coupled with emission of the Γ^{-2}_{15} phonon ($X_o - \Gamma^{-2}_{15}$) by its relative position of 0.08 eV below the X_o emission energy, which is close to the reported value of 0.082 eV for the Γ^{-2}_{15} phonon by Petroff *et al.*[29] Finally, peak 1 was previously assigned to the emission of the Γ^{-2}_{15} and Γ^+_{25} phonons at 1.875 eV.[27] On the other hand, the peak position at 1.891 eV is in good agreement with the energy 1.89 eV calculated by T-Thienprasert and Limpijumnong[16] for optical transition for $(N_2)_{Cu}$. Within the present experiment, however, we cannot conclusively favor one or another assignment for peak 1. The suggested assignments and energy position of the peaks are summarized in Table I.

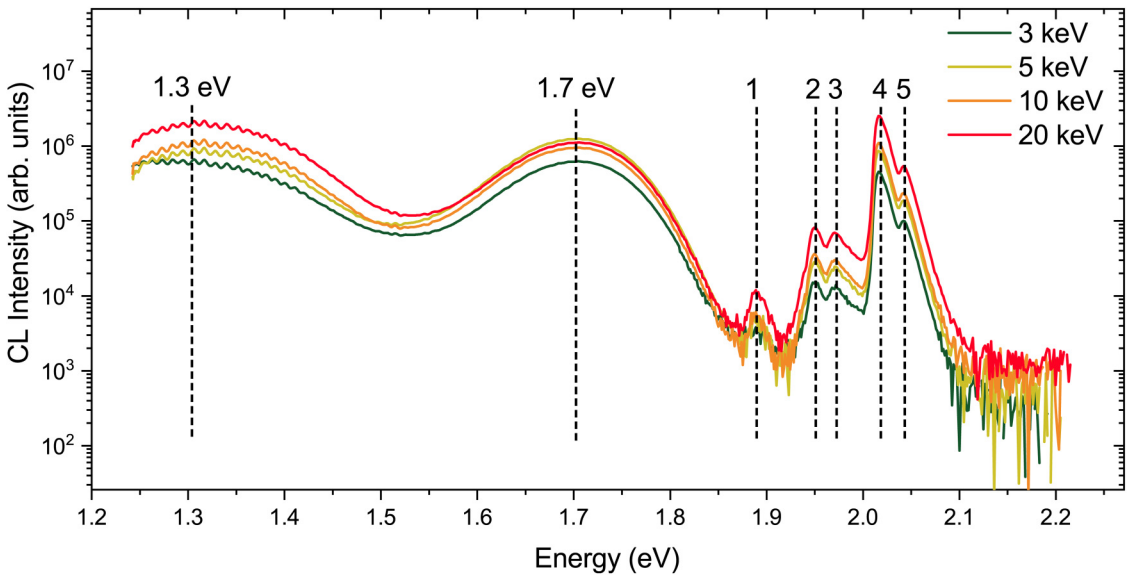

FIG. 2. CL at 80 K in the photon energy range 1.2–2.2 eV recorded for different electron-beam energies: 3, 5, 10, and 20 keV. The assignment of the NBE lines (peaks 1–5) is summarized in Table I.

TDH measurements were conducted to evaluate the electrical transport properties of the Cu_2O crystal (Fig. 3). The measurements reveal p-type conductivity of Cu_2O with a carrier density of $6.7 \times 10^{12}\,cm^{-3}$ and a hole mobility of 48 $cm^2/(Vs)$ at room temperature. One can see that the hole concentration is considerably less compared to nitrogen concentration and the expected concentration of V_{Cu} (around 10^{18}–$10^{20}\,cm^{-3}$).[5] This indicates that the material is highly compensated, presumably with unintentional donor impurities.

As the temperature increases, the hole concentration increases in a closely Arrhenius behavior [Fig. 3(a)]. For a compensated material, the hole concentration can be express by the following relation:[30]

$$p \approx \frac{g_a N_v (N_a - N_d)}{N_d} \exp\left(-\frac{\Delta E_a}{kT}\right), \quad (1)$$

where p is the hole density, N_a is acceptor concentration, N_d is compensating donor concentration, g_a is the degeneracy factor, N_v is the density of states at the valence band, k is Boltzman constant, T is temperature, and E_a is the ionization energy of the acceptor state. One can tentatively identify two slopes of similar magnitudes in Fig. 3(a) that correspond to acceptor activation energies of 0.16 and 0.22 eV. The acceptor concentrations cannot be unambiguously deduced due to incomplete ionization in the investigated temperature range. However, a lower limit estimate can be made for both of the acceptors. This results in the densities $\geq 10^{16}\,cm^{-3}$ for the acceptor at 0.16 eV and $\geq 10^{17}\,cm^{-3}$ for the acceptor at 0.22 eV.

TABLE I. NBE transitions in CL at 80 K and their assignments.

Peak	Energy position (eV)	Assignment
1	1.891	$X_O - \Gamma_{25}^+ - \Gamma_{15}^{-2} \rightarrow \Gamma_7^+$ or $(N_2)_{Cu}$
2	1.950	$X_O + \Gamma_{15}^{-2} \rightarrow \Gamma_7^+$
3	1.974	$X_O + \Gamma_{25}^+ \rightarrow \Gamma_7^+$
4	2.018	$X_O - \Gamma_{12}^- \rightarrow \Gamma_7^+$
5	2.043	$X_O + \Gamma_{12}^- \rightarrow \Gamma_7^+$

One can speculate that the steepening of the slope in the TDH data from 0.16 to 0.22 eV with increasing temperature may not be a manifestation of two different states, but rather a result of other effects. Fitting of the TDH data with a single level to the whole temperature range gives an activation energy of 0.19 eV. However, we tend to assume two distinct levels. This is based on the previous reports on Cu_2O doping with nitrogen:[12,13,31] (1) TDH measurements on undoped Cu_2O reveals acceptors with an activation energy of ≥0.2 eV. (2) The doping results in a decrease in the activation energy down to 0.12 eV. Such behavior suggests two distinct acceptors. The acceptor in the undoped Cu_2O can be assigned to V_{Cu} with the acceptor level at $\sim E_V + 0.25$ eV.[6,7] The acceptor with the activation energy 0.12 eV was attributed to nitrogen, in accordance with previous reports that put the nitrogen level at 0.12–0.18 eV above E_V.[11–13] In line with the literature, we attribute (i) the level at 0.16 eV [Fig. 3(a)] to a nitrogen-related acceptor and (ii) the acceptor with the activation energy 0.22 eV to V_{Cu}.

A sharp increase in carrier concentration is observed at the higher temperature limit of the measurements. This increase corresponds to an activation energy of ~0.4 eV. Two possible explanations can be put forward: (1) there is another deeper acceptor with a level at $\sim E_V + 0.4$ eV and (2) there is an increase in the concentration of shallows acceptors, which is governed by the formation

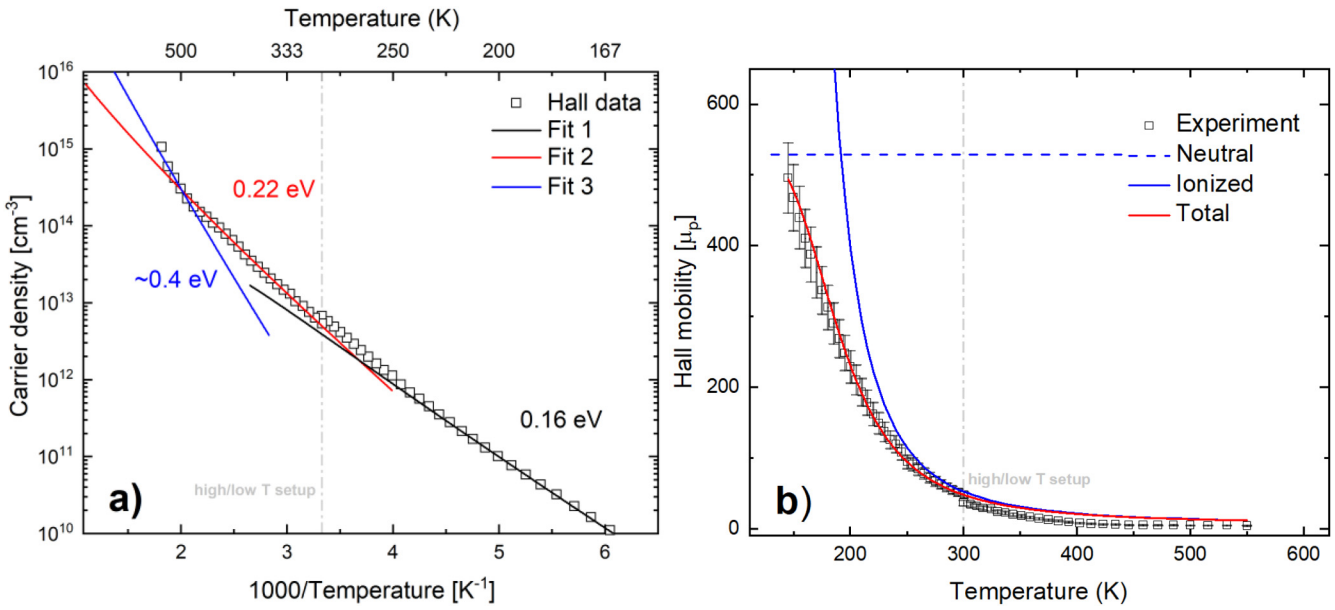

FIG. 3. (a) Hole concentration vs the inverse temperature (squares) as determined by the Hall effect measurement. Exponential fits [Eq. (1)] are indicated with solid lines. (b) Hole mobility as a function of temperature (squares). Curves show the total mobility and contributions from neutral and ionized impurities according to Eq. (3).

energy ~0.4 eV. We favor the former interpretation. First, a similar acceptor has been observed previously by Paul *et al.*[7] and Papadimitriou.[9] Second, the acceptor level at $\sim E_V + 0.4$ eV is consistent with the results of CL measurements, where the 1.7-eV emission can be attributed to a level at $E_C - 1.7$ eV, i.e., at $E_V + 0.47$ eV. We assign this level to $V_{Cu,split}$.

The Hall mobility has a strong dependence on temperature and is shown in Fig. 3(b). Previous studies of hole transport in Cu_2O by Shimada and Masuimo[32] did not result in a consistent picture for hole mobility as a function of temperature: In the low-temperature limit, an acceptable agreement could be made from the combination of phonon LO scattering, acoustical phonon scattering, and neutral impurities. In the higher temperature range, however, another dominating mobility limiting mechanism had to be assumed. To account for the observed rapid decline in mobility, the formation of a metastable self-trapped state has been suggested.[32] A similar rapid decline in mobility is reported by Matsuzaki *et al.*[33] for temperatures above 200 K.

As shown by SIMS, the samples contain a considerable concentration of impurities, with hydrogen concentration (3×10^{19} cm^{-3}) significantly higher than that considered by Shimada and Masuimo.[32] The material is believed to be strongly compensated and contain a significant concentration of both neutral and ionized impurities. It appears to be a reasonable assumption that the main limiting mechanism for hole mobility is scattering at impurities, both neutral and ionized. One can express the total hole mobility, μ, as

$$\mu = \left(\frac{1}{\mu_n} + \frac{1}{\mu_i}\right)^{-1}, \tag{2}$$

where μ_n is the mobility limited by neutral impurities and μ_i is the mobility limited by ionized impurities. Figure 3(a) shows that the hole concentration and, hence, the concentration of ionized impurities, N_i, strongly increases with temperature as an activation-type dependence, $N_i \sim \exp(-E_a/kT)$, where E_a is the activation energy. Both Conwell–Weisskopf and Brooks–Herring approximations (see, for instance, Ref. 34) state that μ_i is inversely proportional to the concentration of ionized impurities and roughly proportional to $T^{3/2}$. One can, thus, express μ_i as $\mu_i = \alpha T^{3/2}/\exp(-E_a/kT)$, where α is the proportionality coefficient. Assuming μ_n is temperature independent, the hole mobility can be expressed as a function of temperature,

$$\mu = \left(\frac{1}{\mu_n} + \frac{\exp(-E_a/kT)}{\alpha T^{3/2}}\right)^{-1}. \tag{3}$$

This expression was fitted to the experimental data in Fig. 3(b). The fitting appears to be satisfactory and yields $\mu_n = 550$ cm^2 V^{-1} s^{-1}, $\alpha = 5.17 \times 10^{-5}$ cm^2 V^{-1} s^{-1} K$^{-3/2}$ and $E_a = 0.14$ eV. Besides, E_a deduced from the mobility data is consistent with the activation energies (0.16–0.22 eV) deduced from the hole concentration data in Fig. 3(a). We conclude that the model can describe the temperature dependence of the mobility.

Figure 4 shows the results of TAS measurements[30] with capacitance [Fig. 4(a)] and conductance [Fig. 4(b)] as functions of temperature for different frequencies and the Arrhenius plot for the emission rates [Fig. 4(c)]. Two dominant electronic levels are evident and manifested as two step-like changes in the capacitance measurements [Fig. 4(a)] and as two peaks in

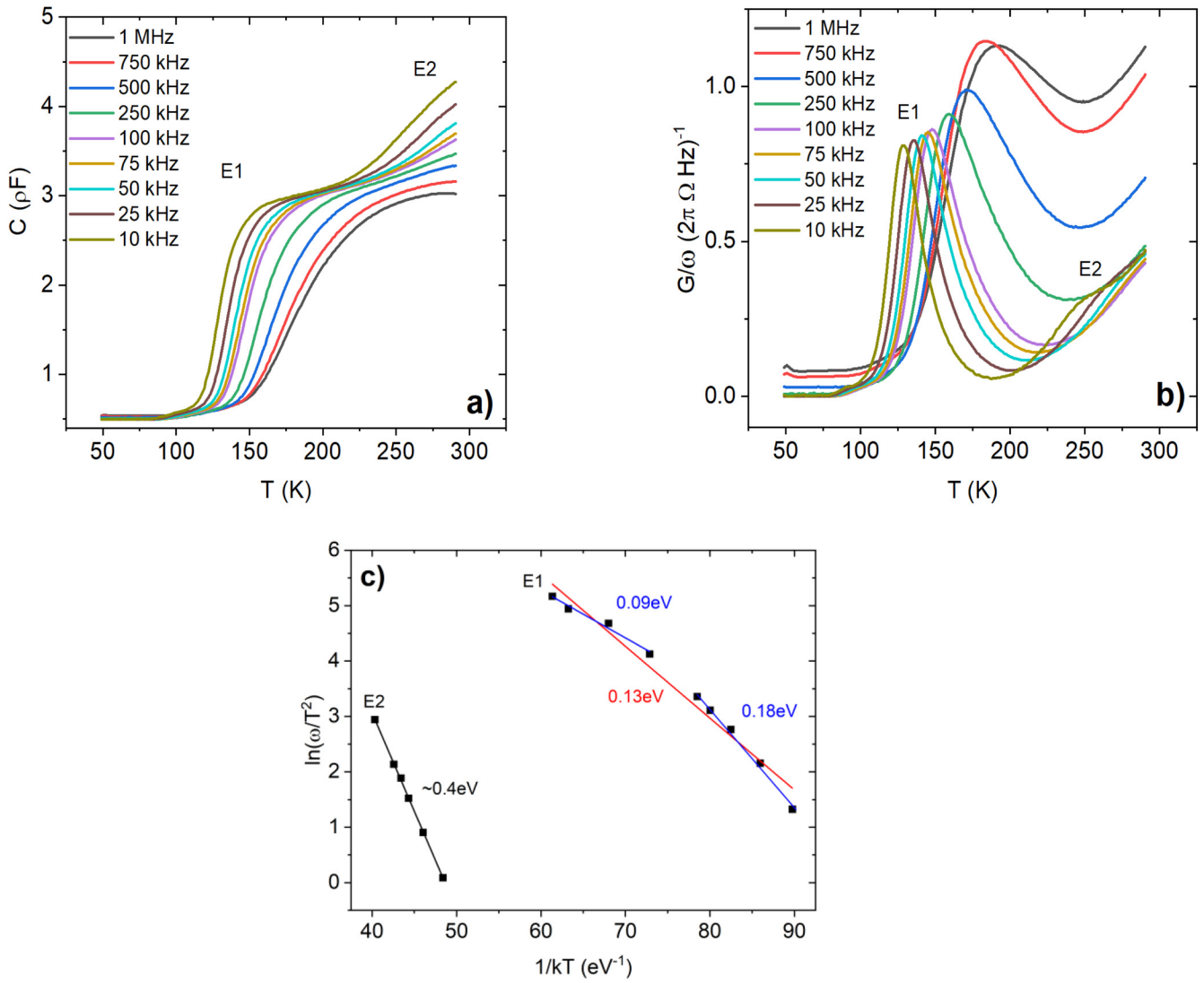

FIG. 4. TAS measurements with capacitance, C (a) and conductance over the angular frequency, G/ω (b) vs temperature for nine different probing frequencies. (c) Arrhenius plot of $\ln(\omega/T^2)$ vs 1/kT for the observed electronic states.

the conductance measurements [Fig. 4(b)]. One level is evident in the 100–200 K range, while another can be observed at >250 K. Arrhenius analysis of the shallower level yield an activation energy of 0.13 eV. One can notice, however, that the emission rate does not demonstrate a clear Arrhenius dependence on the reciprocal temperature. This can be explained by (i) temperature dependence of the capture cross section or (ii) the presence of two overlapping electronic levels. This observation is similar to that for TDH, where two closely positioned acceptor levels are observed [Fig. 3(a)]. Using this interpretation, the two levels are indicated by the additional lines in Fig. 4(c), which results in two levels at 0.09 eV and 0.18 eV above E_V. In line with the interpretation of the TDH data, we assign the level observed with TAS at 0.09 0eV to that observed with TDH at 0.16 eV and attributed to a nitrogen-related acceptor. The level observed with TAS at 0.18 eV is assigned to that observed with TDH at 0.22 eV and identified as the acceptor level of V_{Cu}.

The increasing capacitance and conductance at >250 K indicate the presence of a deeper level [Figs. 4(a) and 4(b)]. This level is particularly visible for lower frequencies. Using the data for these frequencies, the level is estimated to be ~0.4 eV above E_V. This is consistent with the deeper level at 0.4 eV observed by TDH [Fig. 3(a)]. We thus assign this level to $V_{Cu,split}$.

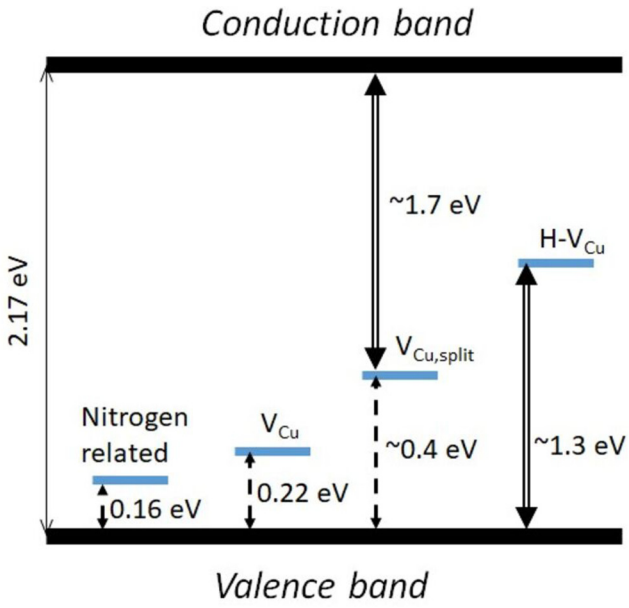

FIG. 5. Schematic illustration of the levels within the bandgap proposed in the present study. Dashed arrows indicate electronic transitions deduced by TDH. The solid double-line arrows denote optical transitions observed by CL.

The proposed assignments of the electronic levels and the corresponding optical transitions are illustrated in Fig. 5. It should be emphasized that the electronic and optical transitions observed in the present study are similar to those observed in other experiments reported in the literature. This suggests that the samples investigated in the present study are representative and comparable to those reported in the literature. Thus, the considerations on the identity of the levels are applicable to identifications reported previously.

IV. CONCLUSION

The dominant electrically active centers and carrier transport in single crystal Cu_2O wafers are studied by several complementary techniques. The measurements reveal electronic levels at around $E_V + 0.16$, $E_V + 0.22$, $E_V + 0.4$, and $E_V + 1.3$ eV. In line with previous identifications, the level at 0.16 eV is assigned to a nitrogen-related acceptor, and the levels at 0.22 and ~0.4 eV are assigned to the acceptor states of V_{Cu} and $V_{Cu,split}$. The level at $E_V + 1.3$ eV is believed to be responsible for the emission line at 1.2–1.3 eV, which is routinely observed in PL and CL measurements. In contrast to the identification as V_{Cu}, normally given in the literature, we tend to attribute this level to the acceptor state of H-V_{Cu}. The origin of another routinely observed emission line at ~1.7 eV is argued to be the acceptor level of $V_{Cu,split}$, as opposed to a widely accepted identification as V_O. In addition, we demonstrate that the mechanism limiting carrier mobility can be described by scattering on neutral and ionized defect centers.

ACKNOWLEDGMENTS

This work was performed within The Norwegian Research Center for Sustainable Solar Cell Technology (FME SUSOLTECH, Project No. 257639/E20). The center is co-sponsored by the Research Council of Norway and its research and industry partners. The Research Council of Norway is acknowledged for the support to the Norwegian Micro- and Nano-Fabrication Facility, NorFab, Project No. 295864, and FUNDAMeNT, Project No. 251131.

AUTHOR DECLARATIONS

Conflict of Interest

The authors have no conflicts to disclose.

DATA AVAILABILITY

The data that support the findings of this study are available from the corresponding authors upon reasonable request.

REFERENCES

[1]C. Malerba, F. Biccari, C. Leonor Azanza Ricardo, M. D'Incau, P. Scardi, and A. Mittiga, Sol. Energy Mater. Sol. Cells **95**, 2848 (2011).
[2]B. K. Meyer, A. Polity, D. Reppin, M. Becker, P. Hering, P. J. Klar, T. Sander, C. Reindl, J. Benz, M. Eickhoff, C. Heiliger, M. Heinemann, J. Blasing, A. Krost, S. Shokovets, C. Muller, and C. Ronning, Phys. Status Solidi B **249**, 1487 (2012).
[3]B. Meyer, A. Polity, D. Reppin, M. Becker, P. Hering, B. Kramm, P. Klar, T. Sander, C. Reindl, C. Heiliger, M. Heinemann, C. Muller, and C. Ronning, *Oxide Semiconductors*, Semiconductors and Semimetals (Elsevier, 2013), p. 201.
[4]T. Minami, Y. Nishi, and T. Miyata, Appl. Phys. Express. **9**, 052301 (2016).
[5]H. Raebiger, S. Lany, and A. Zunger, Phys. Rev. B **76**, 045209 (2007).
[6]D. O. Scanlon, B. J. Morgan, G. W. Watson, and A. Walsh, Phys. Rev. Lett. **103**, 096405 (2009).
[7]G. K. Paul, Y. Nawa, H. Sato, T. Sakurai, and K. Akimoto, Appl. Phys. Lett. **88**, 141901 (2006).
[8]Y. S. Lee, M. T. Winkler, S. C. Siah, R. Brandt, and T. Buonassisi, Appl. Phys. Lett. **98**, 192115 (2011).
[9]L. Papadimitriou, Solid-State Electron. **36**, 431 (1993).
[10]G. P. Pollack and D. Trivich, J. Appl. Phys. **46**, 163 (1975).
[11]S. Ishizuka, S. Kato, T. Maruyama, and K. Akimoto, Jpn. J. Appl. Phys. **40**, 2765 (2001).
[12]J. Li, Z. Mei, L. Liu, H. Liang, A. Azarov, A. Kuznetsov, Y. Liu, A. Ji, Q. Meng, and X. Du, Sci. Rep. **4**, 7240 (2014).
[13]J. Benz, K. P. Hering, B. Kramm, A. Polity, P. J. Klar, S. C. Siah, and T. Buonassisi, Phys. Status Solidi B **254**, 1600421 (2017).
[14]Y. Wang and J. F. Pierson, J. Phys. D: Appl. Phys. **54**, 263002 (2021).
[15]Y. Wang, J. Ghanbaja, D. Horwat, L. Yu, and J. F. Pierson, Appl. Phys. Lett. **110**, 131902 (2017).
[16]J. T-Thienprasert and S. Limpijumnong, Appl. Phys. Lett. **107**, 221905 (2015).
[17]C. Malerba, C. L. Azanza Ricardo, M. D'Incau, F. Biccari, P. Scardi, and A. Mittiga, Sol. Energy Mater. Sol. Cells **105**, 192 (2012).
[18]C. G. Van de Walle and J. Neugebauer, Nature **423**, 626 (2003).
[19]D. O. Scanlon and G. W. Watson, Phys. Rev. Lett. **106**, 186403 (2011).
[20]K. P. Hering, C. Kandzia, J. Benz, B. G. Kramm, M. Eickhoff, and P. J. Klar, J. Appl. Phys. **120**, 185705 (2016).
[21]N. Tabuchi and H. Matsumura, Jpn. J. Appl. Phys. **41**, 5060 (2002).

[22]R. Kumar, K. Bergum, H. N. Riise, E. Monakhov, A. Galeckas, and B. G. Svensson, J. Alloys Compd. **825**, 153982 (2020).
[23]S. Poulston, P. M. Parlett, P. Stone, and M. Bowker, Surf. Interface Anal. **24**, 811 (1996).
[24]J. Bloem, A. J. Van der Houven van Oordt, and F. A. Kröger, Physica **22**, 1254 (1956).
[25]S. V. Gastev, A. A. Kaplyanskii, and N. S. Sokolov, Solid State Commun. **42**, 389 (1982).
[26]M. Zouaghi, B. Prevot, C. Carabatos, and M. Sieskind, Phys. Status Solidi A **11**, 449 (1972).
[27]K. Bergum, H. N. Riise, S. Gorantla, P. F. Lindberg, I. J. T. Jensen, A. E. Gunnæs, A. Galeckas, S. Diplas, B. G. Svensson, and E. Monakhov, J. Phys.: Condens. Matter **30**, 075702 (2018).
[28]K. Shindo, J. Phys. Soc. Jpn. **36**, 1583 (1974).
[29]Y. Petroff, P. Y. Yu, and Y. R. Shen, Phys. Rev. B **12**, 2488 (1975).
[30]P. Blood, *The Electrical Characterization of Semiconductors Majority Carriers and Electron States* (Academic Press Inc., San Diego, CA, 1992).
[31]Y. S. Lee, J. Heo, M. T. Winkler, S. C. Siah, S. B. Kim, R. G. Gordon, and T. Buonassisi, J. Mater. Chem. A. **1**, 15416 (2013).
[32]H. Shimada and T. Masumi, J. Phys. Soc. Jpn. **58**, 1717 (1989).
[33]K. Matsuzaki, K. Nomura, H. Yanagi, T. Kamiya, M. Hirano, and H. Hosono, Appl. Phys. Lett. **93**, 202107 (2008).
[34]D. Chattopadhyay and H. J. Queisser, Rev. Mod. Phys. **53**, 745 (1981).